Gauss and Gauss–Lobatto Element Quadratures Applied to the Incompressible Navier–Stokes Equations.

D. A. Niclasen, H. M. Blackburn
Department of Mechanical Engineering, Monash University, Melbourne, Vic 3168, Australia.

1. Introduction

The Galerkin finite element method of spatially discretising the time–dependent Navier–Stokes equations is attractive when the solution domain is irregular and cannot be conveniently mapped to a rectangular grid. The method overcomes many of the problems associated with finite difference or structured-grid finite volume techniques, and is especially well suited to problems where unstructured mesh techniques can be applied to reduce the number of mesh nodes.

The finite element formalism is usually implemented through the use of quadrature rules to carry out the numerical integration required at element level. Typically, multi-dimensional tensor-product extensions of the one-dimensional Gauss–Legendre (GL) formulae have been used to define the quadrature points and weights for quadrilateral or brick elements. In one space dimension, the GL formulae have the advantage that the order of the quadrature rule can be selected according to the order of the polynomial terms to be integrated such that the full theoretical rate of convergence is achieved. In more than one space dimension, the situation is more complex and the theoretical requirements of quadrature schemes are less well established. For example, rules which establish the sufficiency of tensor-product GL rules for full integration of multidimensional shape-function terms in distorted geometries are known, but other kinds of quadrature schemes are also known to achieve full integration [8].

For certain types of problems GL quadrature can be costly, due to the requirement that the nodal values be interpolated to the quadrature points. This fact, in part, has prompted the adoption of Gauss–Legendre–Lobatto (GLL) rules for Galerkin spectral and spectral element methods [1]. The primary advantage in the use of GLL quadrature is that the quadrature points are located at the nodal points, thus leading to savings since interpolation is no longer required. A secondary advantage is that mass matrix terms are purely diagonal, without resort to any lumping technique, leading to savings in time advancement or integration of forcing terms. A possible disadvantage is the loss of full quadrature accuracy in some cases, however as noted above there are few definitive theoretical or numerical results to guide the adoption of quadrature schemes when the spatial dimension exceeds one.

In this paper, we examine the effect on solution accuracy when GLL quadrature is applied to the advection terms in a finite element approximation to three-dimensional incompressible Navier–Stokes equations where triquadratic velocity shape functions have been used. The rate of convergence in the L_2 (energy) error norm will be

compared for both formulations with both undistorted and distorted brick elements.

2. Time Discretisation

For an incompressible Newtonian fluid, the Navier–Stokes equations are given by

$$\frac{\partial u_i}{\partial t} + \frac{\partial}{\partial x_j}(u_i u_j) = -\frac{1}{\rho}\frac{\partial p}{\partial x_i} + \nu \frac{\partial^2 u_i}{\partial x_j \partial x_j}, \tag{2.1}$$

$$\frac{\partial u_i}{\partial x_i} = 0. \tag{2.2}$$

The time discretisation scheme adopted here is a fractional step method [6], using a 2nd order explicit Adams–Bashforth scheme with a group formulation for the advection terms and a 2nd order implicit Crank–Nicolson scheme for the diffusion terms:

$$\frac{u_i{}^* - u_i{}^{(n)}}{\Delta t} = \frac{\nu}{2}\left[\frac{\partial^2 u_i{}^*}{\partial x_j \partial x_j} + \frac{\partial^2 u_i{}^n}{\partial x_j \partial x_j}\right] - \frac{3}{2}\frac{\partial}{\partial x_j}(u_i{}^n u_j{}^n) + \frac{1}{2}\frac{\partial}{\partial x_j}\left(u_i{}^{(n-1)} u_j{}^{(n-1)}\right) \tag{2.3}$$

$$\frac{\partial^2 p^{(n+1)}}{\partial x_i \partial x_i} = \frac{1}{\Delta t}\frac{\partial u_i{}^*}{\partial x_i} \tag{2.4}$$

$$\frac{u_i{}^{(n+1)} - u_i{}^*}{\Delta t} = -\frac{1}{\rho}\frac{\partial p^{n+1}}{\partial x_i}. \tag{2.5}$$

3. Spatial Discretisation

The discrete equivalent of equation (2.3) under the Galerkin finite element formulation requires at each time step the solution of a set of equations of the form

$$[H]\,\mathbf{u}^* = [H]\,\mathbf{u}^n - \frac{3}{2}[D]\,\mathbf{u}^n + \frac{1}{2}[D]\,\mathbf{u}^{(n-1)}, \tag{3.1}$$

where $[H]$ and $[D]$ are appropriate operator matrices that are assembled from quadratures for each element in the computational domain. For the advection terms these operator matrices correspond to the derivative operator in each of the three coordinate directions. If we consider just one of the advection terms

$$\frac{\partial}{\partial x}(uu), \tag{3.2}$$

we multiply by a weighting function and integrate over an element to get the MWR form

$$\int_\Omega w \frac{\partial}{\partial x}(uu)\, d\Omega. \tag{3.3}$$

This is typical of an integration which is carried out using numerical quadrature. Using the Galerkin formulation, isoparametric elements and a quadrature rule, the equivalent discrete form is

$$\sum_j \sum_A \sum_B \sum_C \phi_i \left[uu\left(J^*_{11}\frac{\partial \phi_j}{\partial e} + J^*_{12}\frac{\partial \phi_j}{\partial n} + J^*_{13}\frac{\partial \phi_j}{\partial r}\right)\right] W_A W_B W_C, \tag{3.4}$$

where the coordinate system has been mapped from (x, y, z) to (e, n, r), and the J^*_{ij} represent the appropriate elements of the inverted Jacobian matrix. The summation over the A, B and C indices takes place at the appropriate quadrature points with discrete weights W.

4. Element Details

The elements used in this study were three-dimensional brick elements, with triquadratic basis functions for velocity and trilinear basis functions for pressure. The use of a lower order of interpolation for pressure is in order to satisfy the Babuska–Brezzi condition [3]. There were a total of 27 velocity nodes and 9 pressure nodes, as shown in Figure 1. The location of the quadrature points for GL quadrature are also shown.

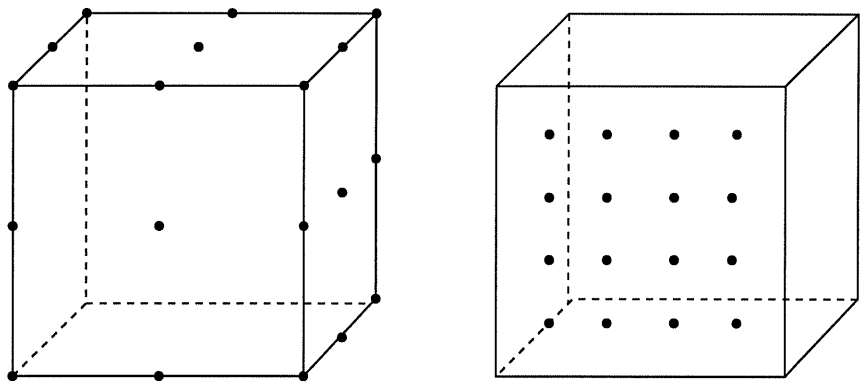

FIGURE 1. Node and quadrature points for triquadratic velocity shape functions on a brick element. (a) Location of element node points, which are the same as the GLL quadrature points (interior point not shown); (b) location of GL quadrature points projected onto one surface.

5. Quadrature Rules

Accuracy results for different kinds of Gauss quadrature rules used to integrate polynomials of different orders in one spatial dimension are well established [1], however as noted in the Introduction the situation is not as clear for a higher number of spatial dimensions.

In order to obtain the full rate of convergence, the quadrature rules used must be capable of integrating exactly all monomials of order $\overline{k} + k - 2m$, where $\overline{k}$ is the order of the highest order monomial present in the element's shape functions, k is the degree of complete polynomial appearing in the element shape functions, and m is the order of the Sobolev space [8, 5]. In tensor-product shape function forms, $\overline{k} = nk$, where n is the number of spatial dimensions. For the elements considered

here, $\overline{k} = 6$, $k = 2$, $m = 1$, so we require a quadrature rule capable of integrating monomials of order 6.

If the number of quadrature points used for a one-dimensional integration is $N+1$, then GL rules exactly integrate polynomials of order $2N+1$, while GLL rules exactly integrate polynomials of order $2N-1$. Since we require integration up to order 6, we need $N = 3$ for GL quadrature, and $N = 4$ for GLL quadrature. In the work reported here the GLL quadrature points coincided with the node points, as is usually the case, meaning that $N = 2$ in the GLL quadrature (corresponding to 3 quadrature/node points). In turn this means that the full rate of convergence may not be achieved, however the degree of any loss of accuracy is not theoretically established.

The major advantage in using GLL quadrature is that the resulting elemental matrices are faster to calculate and require less storage than the equivalent matrices obtained using GL quadrature. Using full GL quadrature, the size of derivative operator matrices to be carried for each element are of the order p^6 (where p is the number of node points in one direction, 3 here), compared to p^4 when GLL quadrature is employed. This leads to a potential reduction in total memory use of around 40% for the code being used in this work.

6. Test Problem

The test problem employed was an analytical solution of the Navier–Stokes equations [2]. The solution is given by

$$\begin{aligned}
u &= -a\left[e^{ax}\sin(ay+bz) + e^{az}\cos(ax+by)\right]e^{-b^2t},\\
v &= -a\left[e^{ay}\sin(az+bx) + e^{ax}\cos(ay+bz)\right]e^{-b^2t},\\
w &= -a\left[e^{az}\sin(ax+by) + e^{ay}\cos(az+bx)\right]e^{-b^2t},\\
p &= \frac{a^2}{2}\Big[e^{2ax} + e^{2ay} + e^{2az} + 2\sin(ax+by)\cos(az+bx)e^{a(y+z)}\\
&\quad +2\sin(ay+bz)\cos(ax+by)e^{a(x+z)}\\
&\quad +2\sin(az+bx)\cos(ay+bz)e^{a(x+y)}\Big]e^{-2b^2t}.
\end{aligned}$$

The values of the constants used were $a = \pi/4$ and $b = \pi/2$, and the solution domain was $[-1,+1]$ in each of the x, y and z directions. Analytical initial conditions were used. The vector field on the surface of the domain can be seen in figure 2.

7. Error Calculations

Numerical values for the L_2 error norm for the velocity field were established by interpolating the solution onto a finer mesh (using 4 GL quadrature points in each direction), and then integrating numerically:

$$L_2 = \| u \| = \left[\sum^{\text{Elements}} \int_\Omega (u_i - \hat{u}_i)(u_i - \hat{u}_i)\, d\Omega\right]^{1/2} \tag{7.1}$$

where $\hat{u}$ is the exact solution. Summation over spatial indices i is assumed.

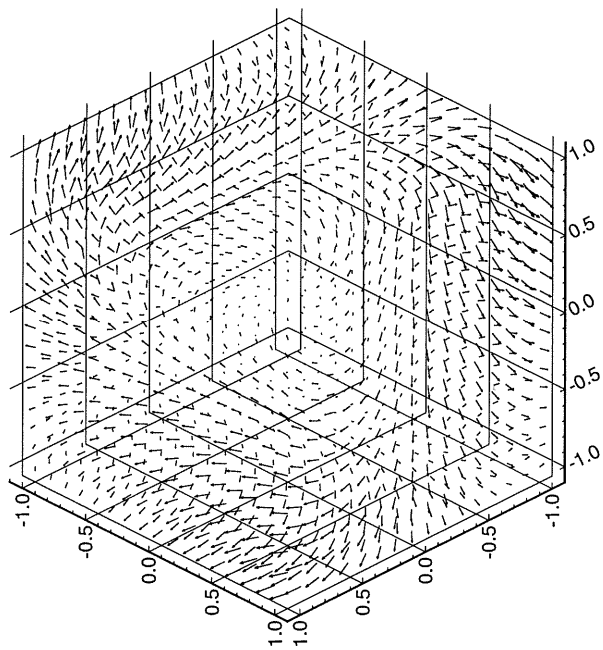

FIGURE 2. Surface vectors for the test problem.

For smooth problems the full rate of spatial convergence is given by $h^{(k+1-m)}$, where h is the element size, k is the degree of complete polynomial in the element shape function, and m is 0 for the L_2 norm [5]. For triquadratic–velocity elements, the expected full rate of spatial convergence is h^3 in the L_2 norm.

8. Convergence Properties for Undistorted Elements

The initial convergence properties were tested in order to confirm that the expected rate of convergence was being achieved. A very small timestep (1.0×10^{-5}) was chosen so that the spatial discretisation errors would dominate the temporal discretisation errors. The simulation was then run for 100 time steps to ensure that the numerical error would stabilise and not be affected by the initial condition. Meshes ranging from 512 to 8000 elements were used. Full GL integration was used for all matrices. The results can be seen in figure 3, indicating that the expected rate of convergence was achieved.

Integration using GLL rules was then applied to the advection term using the same undistorted meshes and the convergence rate examined. The results are given in table 1. From these results, when an undistorted mesh is used there is almost no loss of accuracy when GLL is used. This is similar to previously documented behaviour for mass lumping with undistorted elements [7]. The good performance in this case is however expected, owing to the fact that the lack of distortion leads to the highest-order terms requiring integration to be the same as for one spatial dimension, where three GLL points are sufficient to attain full quadrature accuracy in this case.

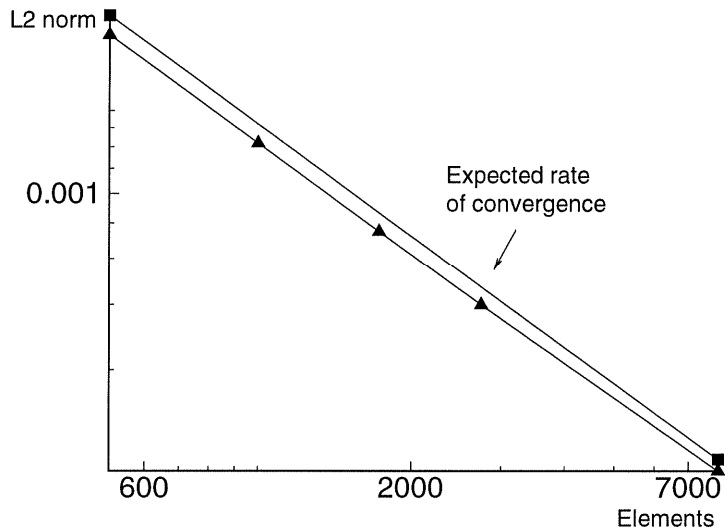

FIGURE 3. Convergence rate in the L_2 norm for undistorted elements and full Gauss Legendre quadrature for all terms.

TABLE 1. L_2 error norm for undistorted meshes showing effect of quadrature rules for advection terms.

Mesh size	Total Elements	GL integration	GLL integration
$8 \times 8 \times 8$	512	0.001595	0.001602
$10 \times 10 \times 10$	512	0.000818	0.000822
$12 \times 12 \times 12$	1000	0.000475	0.000476
$14 \times 14 \times 14$	2744	0.000300	0.000301
$20 \times 20 \times 20$	8000	0.000107	0.000107

9. Convergence Properties for Distorted Elements

The principal motivation for using finite element methods rather than the computationally less expensive finite difference or finite volume methods lies in is its advantages when applied to complex domains. This in turn means that element shapes are often distorted rather than rectangular prismatic, leading to higher-order monomials and possibly some loss in quadrature accuracy. In order to investigate the effect that element distortion would have when GLL integration was used, the mesh was distorted by adding random 'noise'. Different levels of noise were added by setting a 'noise factor', which was defined as the maximum distance that a node could be moved as a fraction of the element length. Noise factors ranging from 0.0001 to 0.1 were used. Movement of nodes on the outside of the domain was not allowed so that the extents of the domain remained the same as for the undistorted case.

TABLE 2. L_2 error norm for different levels of mesh distortion.

Noise Factor	GL	GLL
$8 \times 8 \times 8$ elements		
0.0001	0.001599	0.001606
0.001	0.001830	0.001838
0.01	0.008934	0.008938
0.1	0.093899	0.093912
$10 \times 10 \times 10$ elements		
0.0001	0.000841	0.000844
0.001	0.002039	0.002042
0.01	0.019340	0.019355
0.1	0.066164	0.066345
$12 \times 12 \times 12$ elements		
0.0001	0.000480	0.000481
0.001	0.000782	0.000784
0.01	0.006259	0.006261
0.1	0.075527	0.075816
$14 \times 14 \times 14$ elements		
0.0001	0.000306	0.000307
0.001	0.000648	0.000649
0.01	0.005782	0.005785
0.1	0.066164	0.066236

Mesh sizes ranged from 8 elements in each direction to 14 elements in each direction. Solutions were obtained using GL quadrature for all terms and GLL quadrature for the advection terms only. The L_2 error norm for each case tested is given in table 2. The error norm as a function of the mesh distortion level is shown in figure 4. The error norm is higher for the more refined meshes in some cases as the level of mesh distortion is effectively greater.

The results from table 2 showed that no loss of accuracy occurred when GLL quadrature was applied to the advection term. The results are still not conclusive however as the test problem used is diffusion dominant. This may mean that a lower accuracy in the advection term is being masked by the size of the diffusion term. A further series of tests are required using a problem which is advection dominated, or on a linear advection problem. This will allow the advection term to be isolated from the other terms in the Navier–Stokes equations.

10. Conclusions

For the cases presented, the use of GLL quadrature for the calculation of the advection term matrix operators did not lead to any reduction in solution accuracy. Given the substantial savings in memory usage which are possible using this approach, the method looks promising. In order to further investigate this approach, it is necessary

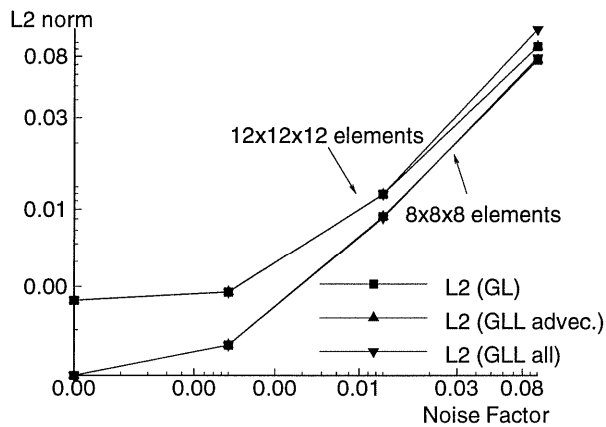

FIGURE 4. Variation of L_2 error norm for different quadrature schemes with changing mesh distortion levels.

to isolate the effects of the advection term from the other terms in the equations, as the test case presented was diffusion dominated. Further work is planned in this area.

References

[1] Canuto C., Hussaini M. Y., Quarteroni A., & Zang T. A., *Spectral Methods in Fluid Dynamics*, Springer, 1988.

[2] Ethier C. R, & Steinman D. A., Exact fully-3D Navier–Stokes solutions for benchmarking, *Int. J. Num. Meth. Fluids*, **19**, 1994, 369–375.

[3] Fortin M., Old and new finite elements for incompressible flows,*Num. Meth. Fluids*,**1**, 1981, 347–364.

[4] Gresho P. M., Lee R. L. & Sani R. L., Advection-dominated flows, with emphasis on the consequences of mass lumping, in *Finite Elements in Fluids*, Wiley, 1978.

[5] Hughes T. J. R., *The Finite Element Method*, Prentice–Hall, 1987.

[6] Kim J. & Moin P., Application of a fractional-step method to incompressible Navier–Stokes equations, *J. Comp. Phys*, **59**, 1985, 308–323.

[7] Niclasen, D. A. & Blackburn, H M., A comparison of mass lumping techniques for the two-dimensional Navier–Stokes equations, in *12th A/Asian Fluid Mech. Conf.*, Sydney, 1995, 731–734.

[8] Strang, G & Fix, G. J. *An Analysis of the Finite Element Method*, Prentice–Hall, 1973.